Journal of
Synchrotron
Radiation
ISSN 0909-0495

Received 24 January 2005
Accepted 8 April 2005

Lowest limit for detection of impurity concentration in semiconductors by fluorescence XAFS: resonant Raman scattering and angle dependence

Y. Takeda,* H. Ofuchi, H. Kyouzu, R. Takahashi and M. Tabuchi

Department of Materials Science and Engineering, Graduate School of Engineering, Nagoya University, Furo-cho, Chikusa-ku, Nagoya 464-8603, Japan. E-mail: takeda@numse.nagoya-u.ac.jp

The lowest limit for detection (LLD) of the impurity concentration doped in semiconductors in the case of fluorescence XAFS measurements has been investigated as a function of the matrix of the impurity and the geometry of the measurement. When the impurity concentration is very low and other background noise is well suppressed, X-ray resonant Raman scattering by the constituent atoms of the matrix remains as a major background for the fluorescence-detected XAFS measurement. For example, in the fluorescence-detected XAFS measurement for Er-doped semiconductors at the Er L_{III}-edge, the LLD of the Er concentration was about 5×10^{14} to 1×10^{15} cm^{-2} for GaAs and GaP, and lower than 1×10^{14} cm^{-2} for InP. The resonant Raman scattering of Ga atoms in the host semiconductor determines the LLD.

© 2005 International Union of Crystallography
Printed in Great Britain – all rights reserved

Keywords: impurity; XAFS; semiconductors; resonant Raman.

1. Introduction

In most semiconductors used for device applications, impurity atoms play very important roles in controlling the properties of the semiconductor. The properties of semiconductors containing impurity atoms are naturally related to the local structures around the impurity atoms. For example, impurity atoms which replace a lattice site and those occupied at interstitial sites behave very differently, electrically and/or optically. The local structures depend on the concentration of the impurity atoms. In heavily doped semiconductors the impurity atoms tend to segregate and to form complex structures and precipitates. In many devices the active regions are doped at concentrations of 1×10^{18} to 5×10^{18} cm^{-3} in order to locate the impurity atoms on the lattice sites and to make them active as intended. Therefore, the local structures of the impurity atoms at concentrations of 1×10^{18} to 5×10^{18} cm^{-3} are of interest for semiconductor physics and engineering in order to understand the behavior of the impurity atoms and to control the properties.

Erbium is one of the important impurity atoms. It has sharp and temperature-insensitive intra-4*f*-shell luminescence at 1.54 µm, which corresponds to the minimum transmission loss of silica-based fibers. Thus, Er-doped semiconductors have been intensively studied in recent years (Fujiwara *et al.*, 2000, and references therein). In our studies we have used fluorescence XAFS (X-ray absorption fine structure) measurements to investigate the local structure around Er atoms. Especially in Er-doped InP, we have succeeded in measuring and analyzing the local structures of Er atoms to a lowest number of 3×10^{12} in an X-ray spot size of 1.5 mm × 1.0 mm (this number corresponds to a concentration of 2×10^{18} cm^{-3} in a 1 mm-thick layer) (Ofuchi *et al.*, 1998). However, over the course of XAFS measurements of low Er concentrations in various semiconductors we found that the background level of fluorescence XAFS spectra depended on the matrix semiconductors themselves, in which Er atoms were doped. Fig. 1 shows the raw data of Er $L\alpha$ fluorescence-detected XAFS spectra. Er atoms are doped in GaP (*a*) and InP (*c*), and Er and O atoms are doped in GaAs (*b*). In the pre-edge region of the spectrum of Er-doped InP (*c*), the background curve decreased with an increase in excitation energy, as is the case for normal fluorescence-detected XAFS. However, in the spectra of Er-doped GaP (*a*) and GaAs (*b*), both the pre-edge and the post-edge background curves increase. The background limits the lowest Er concentration that can be used as the XAFS data for the analysis. We need to investigate the strange behavior of the background spectra of Er in GaP and GaAs and to lower the background.

In this work, the lowest limit for detection (LLD) of the impurity concentration doped in semiconductors for fluorescence XAFS measurements is investigated as a function of the matrix and the geometry of the measurement. It is revealed that X-ray resonant Raman scattering in the matrix semiconductors is the limiting factor.

2. Experimental

Measurements were performed at beamline BL12C of the Photon Factory in Tsukuba, Japan, using synchrotron radia-

tion from a 2.5 GeV storage ring. All of the optics and detecting systems for the fluorescence and scattered X-rays were the same as those for fluorescence EXAFS measurements, *i.e.* a Si(111) double-crystal monochromator and bent cylindrical mirror, which were used to monochromate and focus the incident X-ray beam, and 19 elements of a Ge solid-state detector (SSD) to detect the fluorescence and scattered X-rays (Nomura & Koyama, 1996; Nomura, 1998). The fluorescence and scattered X-ray spectra were measured as a function of the sample, the incident X-ray energy, the geometry of the samples and the detector angle. The incident X-ray angle was fixed at $\sim 3^{\circ}$.

3. Results and discussion

Fig. 2 shows the signal to background (S/B) intensity ratio for Er-doped GaP, Er- and O-doped GaAs and Er-doped InP as a function of incident X-ray energy. The sheet impurity concentration was 2×10^{14} cm^{-2} for all of the samples. Although in all of the samples the sheet impurity density was the same, the S/B ratios in Er-doped GaP and Er-doped GaAs were 30–50% lower compared with those in Er-doped InP. In addition, the S/B ratios in Er-doped GaP and Er-doped GaAs decreased with an increase in the incident X-ray energy. However, in the Er-doped InP the S/B ratio increased slightly.

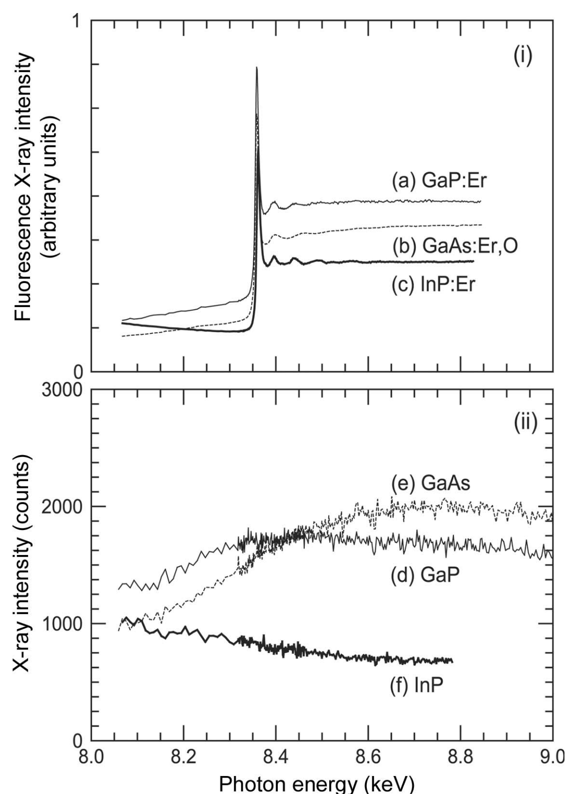

Figure 1
(i) Measured XAFS spectra of (*a*) Er-doped GaP (thin solid line), (*b*) Er- and O-doped GaAs (dotted line) and (*c*) Er-doped InP (bold solid line) at the Er $L_{\rm III}$ edge. (ii) Measured XAFS spectra of (*d*) GaP (thin solid line), (*e*) GaAs (dotted line) and (*f*) InP (bold solid line) at the Er $L_{\rm III}$ edge.

Fig. 3(i) shows X-ray intensity distributions for (*a*) Er-doped GaP, (*b*) Er- and O-doped GaAs and (*c*) Er-doped InP. For all the samples the Er concentration was 2×10^{18} cm^{-3} (the sheet impurity concentration was 2×10^{14} cm^{-2}). The incident X-ray energy was 8.854 keV (the $L_{\rm III}$ absorption edge of Er is 8.360 keV). As shown in Fig. 3, in Er-doped GaP and Er-doped GaAs the Er $L\alpha$ peak was almost buried in the background X-rays which are distributed widely in energy, and was at its highest at around the Er $L\alpha$ energy; in Er-doped InP, however, it was clearly distinguished from the background.

To observe the background spectra in nominally undoped semiconductors the X-ray intensity distributions of GaP (Fig. 3*d*), GaAs (Fig. 3*e*), InP (Fig. 3*f*) and InAs (Fig. 3*g*) were measured. It can be clearly seen that the background X-radiation in GaP and GaAs is high and has a peak near the tail of the elastically scattered X-rays, but lower in InAs and has a wider dip in InP. Those background peaks located around the Er $L\alpha$ energy in GaP and GaAs, and the dip of the background in InP, are close to the Er $L\alpha$ energy.

In order to understand the origin of the broad background, especially in GaP and GaAs, we measured the X-ray intensity distributions of GaAs over a wider range at different incident X-ray energies. As shown in Fig. 4, the peak of the background moved with the change in incident X-ray energy, and the energy difference between the background and the incident X-ray peaks was about 1.150 keV, which corresponded to the energy of Ga *L* and/or As *L*. Therefore, the origin of the background is considered to be the X-ray resonant Raman scattering of Ga and/or As (Hamalainen *et al.*, 1989; Jaklevic *et al.*, 1988; Udagawa *et al.*, 1994). From the spectra in Fig. 3, however, the X-ray resonant Raman scattering of As is low, as observed in the case of InAs. Thus, it is concluded that the

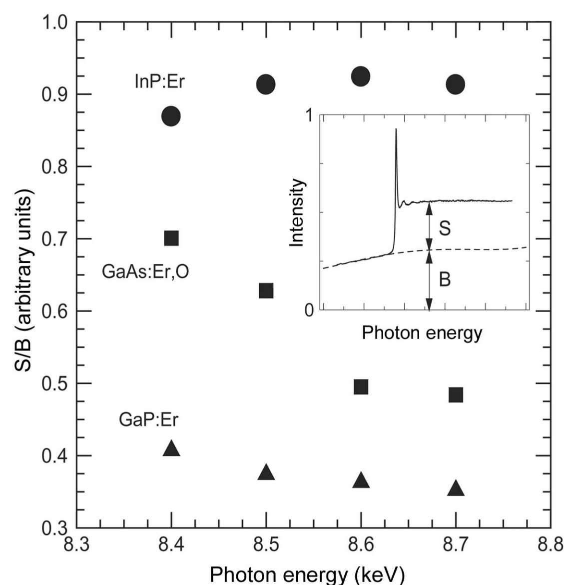

Figure 2
Signal to background intensity ratio for samples of Er-doped GaP (triangles), Er- and O-doped GaAs (squares) and Er-doped InP (circles) as a function of the incident X-ray energy. The inset shows the signal (S) and background (B) intensity in the XAFS spectrum for Er- and O-doped GaAs.

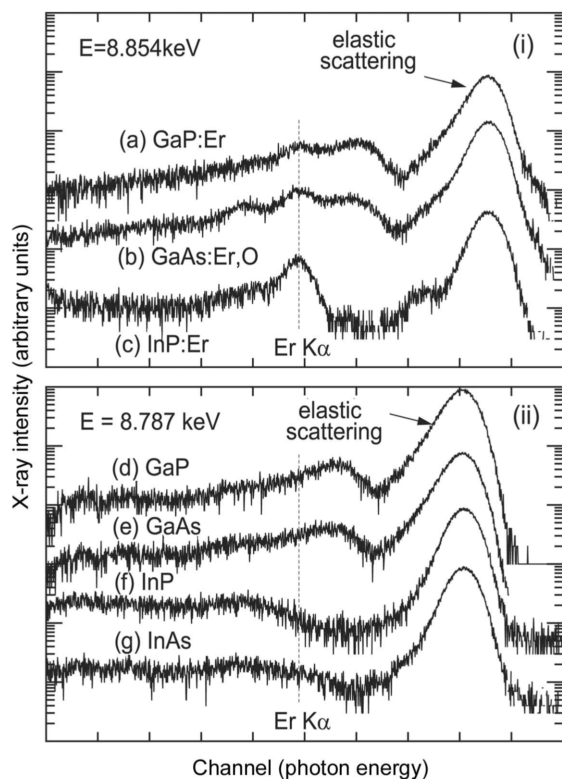

Figure 3
(i) X-ray intensity distributions for samples of (*a*) Er-doped GaP, (*b*) Er- and O-doped GaAs and (*c*) Er-doped InP. The Er $L\alpha$ peak is almost buried in the background in Er-doped GaP and Er-doped GaAs, but is clearly observed in Er-doped InP. (ii) X-ray intensity distributions for the nominally undoped samples of (*a*) GaP, (*b*) GaAs, (*c*) InP and (*d*) InAs. The background X-rays below the elastically scattered X-rays is high and has a peak in GaP and GaAs, but low in InP and InAs and has a dip in InP.

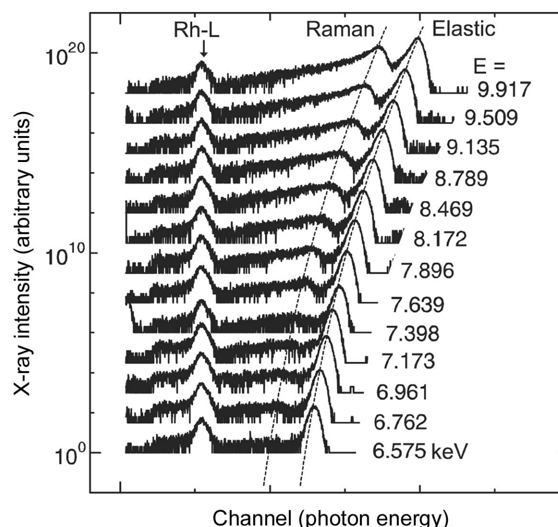

Figure 4
Change in the X-ray intensity distributions for GaAs with a change in the incident X-ray energy. Each spectrum is vertically shifted by a factor of $10^{1.5}$ for clarity. The incident X-ray energy (E) was varied in the range from 6.575 to 9.917 keV. Dotted lines indicate the peak positions of Raman and elastic scattering. The Rh $L\alpha$ peaks derive from the Rh-coated bent cylindrical mirror at the beamline.

main origin of the background for the Er-doped GaAs and GaP in Fig. 1(i) is the X-ray resonant Raman scattering of Ga in GaAs and GaP.

Fig. 5 shows an example of the geometry dependence of the Er $L\alpha$ fluorescence, X-ray resonant Raman scattering and elastic scattering intensity for an Er-doped GaAs sample measured using incident X-rays of 8.790 keV. The geometry of the measurement is illustrated in Fig. 5(*a*). As shown in Fig. 5(*b*), the elastic scattering and the X-ray resonant Raman scattering intensity increased with an increase in the detector angle θ, as expected, and were almost proportional to $\sin^2\theta$ and $1/\cos\theta$, respectively. However, the fluorescence X-ray intensity was almost independent of the detector angle θ. The fluorescence X-rays radiate from the Er-doped GaAs layer of thickness 2 µm, while the X-ray resonant Raman scattering radiates from both the Er-doped GaAs layer and the GaAs substrate. Thus, the attenuation of the Er $L\alpha$ fluorescence by absorption in the GaAs matrix is less than 30%, which is smaller than that of the X-ray resonant Raman scattering. Therefore, it is considered that the variation of the fluorescence X-ray intensity is very small for the variation of the detector angle θ. These results indicate that background intensity in the fluorescence XAFS spectra is minimum when the detector angle is zero.

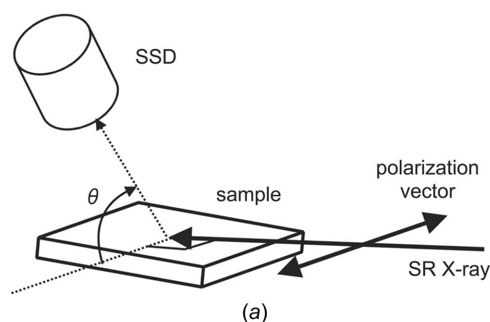

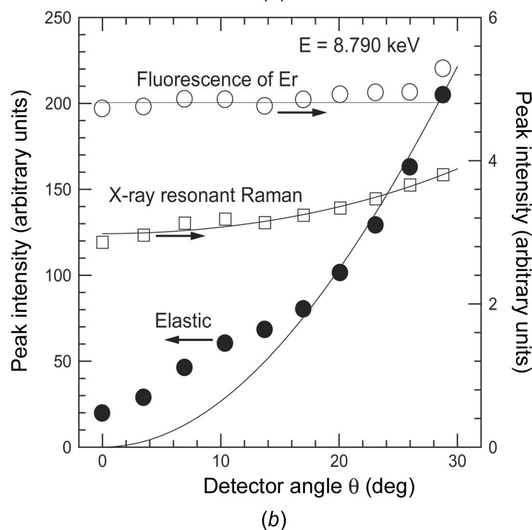

Figure 5
(*a*) Geometry of the sample and the solid-state detector (SSD) for measuring the angle dependence of the fluorescence and scattered X-rays. The SSD makes an angle θ with the polarization vector of the incident X-ray beam. (*b*) Angle dependence of the fluorescence (white circles), X-ray resonant Raman scattering (squares) and elastic scattering intensity (black circles) from an Er-doped GaAs sample. The incident X-ray energy was fixed at 8.790 keV.

3.1. LLD of Er-doped semiconductors

We express the statistical LLD of a specific signal in EXAFS analysis as

$$S > 10B^{1/2}, \qquad (1)$$

where S represents the signal intensity and B represents the background intensity, in which the relative standard deviation is within 10% (Currie, 1968). For Er-doped semiconductors, the signal and the background intensities correspond to the intensity of the Er $L\alpha$ fluorescence of the Er-doped semiconductor and the scattered X-ray intensity for the undoped semiconductor, respectively. Fig. 1(ii) shows the raw data of the scattered X-ray intensity for (*a*) GaP, (*b*) GaAs and (*c*) InP as functions of the incident X-ray energy. The scattered X-rays were detected at 6.95 keV, which corresponded to the energy of the Er $L\alpha$ fluorescence. The X-ray intensity for GaP and GaAs was 1500–2000 counts s^{-1} per element of SSD, and that for InP was 700–800 counts s^{-1}. It is found that the background intensities for GaP and GaAs are about three times as large as for InP. When the EXAFS spectrum is measured for 200 s per incident X-ray energy point by using ten elements of the SSD (the usual measurement conditions for Er-doped semiconductors), the background intensities for GaP and GaAs are 3×10^6 to 4×10^6 counts. Under these measurement conditions, the statistical LLD of the fluorescence X-ray intensity of Er doped in GaAs and GaP is 1.7×10^4 to 2.0×10^4 counts, and that in InP is 1.2×10^4 to 1.3×10^4 counts. It is expected that the statistical LLD of Er doped in GaP and GaAs is 1.3 to 1.7 times as large as that for Er doped in InP. Fig. 6 shows the intensity of Er $L\alpha$ fluorescence for Er-doped GaP, Er- and O-doped GaAs and Er-doped InP as a function of sheet density of Er. The intensity of the Er $L\alpha$ fluorescence was estimated by the background intensity under the above measurement conditions. The sheet density of Er expected from the statistical LLD is 1×10^{13}–3×10^{13} cm^{-2}. In our EXAFS analysis for Er-doped semiconductors, however, the experimentally obtained LLD for Er- and O-doped GaAs and Er-doped GaP is about 5×10^{14}–1×10^{15} cm^{-2} (intensity of Er $L\alpha$ fluorescence, 3×10^5 counts), and that for Er-doped InP is 1×10^{14} cm^{-2} (intensity of Er $L\alpha$ fluorescence, $\sim 1 \times 10^5$ counts). It is found that the experimental LLD is 10 to 100 times as large as that found statistically. The EXAFS oscillation $\chi(k)$ is subtracted from the fluorescence X-ray intensity spectra as shown in Fig. 1. The subtracted EXAFS oscillation $\chi(k)$ contains errors not only in the fluorescence X-ray intensity but also in the background intensity. Moreover, the EXAFS oscillation $\chi(k)$ is multiplied by some power of wavenumber k to $k^n\chi(k)$ as a weighting scheme, resulting in enhancing the errors in the EXAFS spectra. Thus, it is considered that the added errors for the EXAFS spectra cause the difference between the experimental and the statistical LLD.

The lowest impurity concentration which can be measured by the fluorescence-detected XAFS is limited by the X-ray resonant Raman scattering in some semiconductors, and it depends on the combination of matrix, absorption-edge and fluorescence energy of the impurity. Experimentally, it is necessary that the S/B ratios in the Er-doped III–V semiconductors at incident X-ray energies of 8.7 keV are about 1. The limits can be roughly estimated from our experiments in the energy range 6.8−9.0 keV, and are listed in Table 1).

Table 1
Roughly estimated lowest limits of impurity concentrations in major semiconductors for fluorescence EXAFS measurements in the energy range 6.8–9.0 keV (L: $<1 \times 10^{14}$ cm^{-2}; M: 5×10^{14} to 1×10^{15} cm^{-2}).

Matrix	Lowest limit
GaP	*M*
GaAs	*M*
InP	*L*
InAs	*L*
K-edge	Co–Cu
L-edge	Eu–Tm

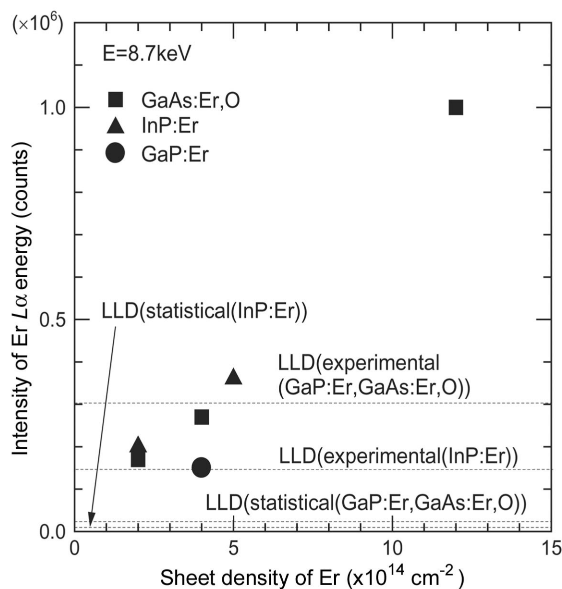

Figure 6
Signal intensity for Er-doped GaP (circles), Er- and O-doped GaAs (squares) and Er-doped InP (triangles) as a function of sheet density of Er. The measurement time is for 200 s per incident X-ray energy point using ten elements of a SSD. The incident X-ray energy was fixed at 8.70 keV. The dotted lines show the statistical and experimental lowest limit of detection (LLD).

4. Conclusions

The lowest limits of the impurity concentrations doped in semiconductors for fluorescence-detected XAFS measurements have been investigated as a function of the matrix and the geometry of the measurements. When the impurity concentration is very low and other background noises are eliminated, the X-ray resonant Raman scattering of the constituent atoms of the matrix remains as a major background noise for the XAFS measurement. For example, in order to conduct fluorescence-detected XAFS measurements at the Er L_{III} edge, the lowest limit of the Er concentration was

about 5×10^{14} to 1×10^{15} cm^{-2} for GaAs and GaP, and lower than 1×10^{14} cm^{-2} for InP.

The authors would like to thank Professor T. Iwazumi at the Photon Factory, KEK, Tsukuba, Japan, for helpful discussions. This work was performed as part of a project (Project No. 95G221 and 97G052) accepted by the Photon Factory Program Advisory Committee.

References

Currie, L. A. (1968). *Anal. Chem.* **40**, 586–593.

Fujiwara, Y., Ofuchi, H., Tabuchi, M. & Takeda, Y. (2000). *Growth Condition Dependences of Optical Properties of Er in InP and Local Structures*, in *InP and Related Compounds*, edited by M. O. Manasreh, pp. 251–311. Amsterdam: Gordon and Breach.

Hamalainen, K., Manninent, S., Suortti., P., Collins, S. P., Cooper, M. J. & Laundy, D. (1989). *J. Phys. Condens. Matter*, **1**, 5595–5964.

Jaklevic, J. M., Giauque, R. D. & Thompson, A. C. (1988). *Anal. Chem.* **60**, 482–484.

Nomura, M. (1998). KEK Report 98–4. KEK, Tsukuba, Ibaraki, Japan.

Nomura, M. & Koyama, A. (1996). KEK Report 95–15. KEK, Tsukuba, Ibaraki, Japan.

Ofuchi, H., Kawamura, D., Tsuchiya, J., Matsubara, N., Tabuchi, M., Fujiwara, Y. & Takeda, Y. (1998). *J. Synchrotron Rad.* **5**, 1061–1063.

Udagawa, Y., Hayashi, H., Tohji, K. & Mizushima, T. (1994). *J. Phys. Soc. Jpn*, **63**, 1713–1720.